arXiv:1401.6879v2 [hep-ph] 6 Feb 2014

Constraints on the parameters of axion from measurements of thermal Casimir-Polder force

V. B. Bezerra,[1] G. L. Klimchitskaya,[2,3] V. M. Mostepanenko,[2,3] and C. Romero[1]

[1]*Department of Physics, Federal University of Paraíba, C.P.5008, CEP 58059–970, João Pessoa, Pb-Brazil*

[2]*Central Astronomical Observatory at Pulkovo of the Russian Academy of Sciences, St.Petersburg, 196140, Russia*

[3]*Institute of Physics, Nanotechnology and Telecommunications, St.Petersburg State Polytechnical University, St.Petersburg, 195251, Russia*

Abstract

Stronger constraints on the pseudoscalar coupling constants of an axion and axion-like particles with a proton and a neutron are obtained from measurements of the thermal Casimir-Polder force between a Bose-Einstein condensate of ^{87}Rb atoms and a SiO_2 plate. For this purpose the additional force acting between a condensate cloud and a plate due to two-axion exchange is calculated. The obtained constraints refer to the axion masses from 0.1 meV to 0.3 eV which overlap with the region from 0.01 meV to 10 meV considered at the moment as the most prospective.

PACS numbers: 14.80.Va, 12.20.Fv, 14.80.-j

I. INTRODUCTION

Axions have attracted considerable attention of elementary particle physicists and cosmologists over many years (for a recent review see Ref. [1]). Although up to the present this particle has not been discovered experimentally, its possible parameters, such as mass and interaction constants with ordinary elementary particles, are the subject of much investigation. This is because the axion has become a crucial element of quantum chromodynamics, which proved to be the fundamental theory of strong interactions in agreement with numerous experimental results and part of the standard model. It is common knowledge, however, that in general terms the formalism of quantum chromodynamics leads to prediction of strong *CP* violation and large electric dipole moment for the neutron in contradiction with the facts. To avoid this contradiction, Peccei and Quinn [2] introduced an additional global symmetry U(1) which is broken both spontaneously and explicitly in the Lagrangian. As was shown by Weinberg [3] and Wilczek [4], this results in the appearance of a light pseudoscalar particle called the *axion*. More recently, axions were widely discussed in astrophysics and cosmology as possible constituents of dark matter [5–10]. In the process different kinds of axion fields have been used, specifically, introduced in string theory. Though not all of them solve the problem of strong *CP* violation, they have generally similar properties and are axion-like particles. Keeping this in mind, we will nevertheless use axion and axion-like particles more or less synonymously.

The interaction of axion with photon is characterized by the coupling constant $g_{a\gamma}$ and is used in many experimental searches for this particle. The axion can also interact with electrons, protons and neutrons by means of pseudoscalar (scalar) couplings [11] with respective coupling constants $g_{ae,p(s)}$, $g_{ap,p(s)}$, and $g_{an,p(s)}$. The constraints on $g_{a\gamma}$ and $g_{ae,p(s)}$ were obtained in different experiments for various ranges of the axion mass (see Refs. [12–15] for a review). For example, rather strong constraint on $g_{a\gamma}$ was found from the search of solar axions with masses from 0.39 eV to 0.64 eV by using the CERN axion solar telescope [16]. The restrictive limits on $g_{a\gamma}$ follow from astrophysics by considering gravitationally bound systems of stars of approximately the same age (the so-called *globular clasters*). These limits are applicable to axions of larger masses $m_a \lesssim 30\,\mathrm{keV}$ [17]. Some constraints on $g_{ae,p}$ were obtained from the study of processes with axions in stellar plasmas, such as the Compton process and the electron-positron annihilation with emission of an axion [18, 19].

Below, we deal with the constraints on m_a and the coupling constants $g_{ap,p}$, $g_{an,p}$ characterizing pseudoscalar interaction of axion-like particles with nucleons. Previously, constraints on these constants were obtained from the search of the Compton-like process for solar axions and from the observation of the neutrino burst of supernova 1987A [13]. Many constraints were obtained in cosmology taking into account that axions should be produced in the early Universe and contribute to dark matter [20]. Specifically, cosmological data exclude axions with mass $m_a > 0.7\,\mathrm{eV}$ because they would provide a too large contribution to the hot dark matter [21]. Such kind limits, however, typically refer to specific couplings in some axion models and may be not applicable to all axion-like particles.

Broadly speaking, constraints on the parameters of an axion obtained from astrophysics and cosmology are also more model-dependent in comparison to table-top laboratory experiments [22, 23]. In Refs. [24–26] it was suggested to use laboratory experiments testing the validity of the weak equivalence principle [26, 27] and of the inverse square law [28] for constraining the coupling constants $g_{ap,p}$ and $g_{an,p}$ in the limit of zero axion mass m_a. Later, the results of Refs. [24–26] were extended [29] to the more realistic case of massive axions. From the gravitational experiments of Eötvos- and Cavendish-type rather strong constraints on $g_{ap,p}$ and $g_{an,p}$ were obtained [29] for the axion masses $m_a \leq 9.9\mu\mathrm{eV}$. Further work on constraining interactions mediated by light pseudoscalar particles from the laboratory experiments was done in Ref. [30] by using a torsion pendulum containing polarized electrons interacting with an unpolarized matter. From the improved setup of this kind, strong constraints were obtained [31, 32] on the product of the coupling constants $g_{aN,s}g_{ae,p}$, where N denotes either a proton or a neutron, under the assumption that $g_{ap,s} = g_{an,s}$. The constraints of Refs. [31, 32] extend to a broad range of axion masses from $10\,\mu\mathrm{eV}$ to $10\,\mathrm{meV}$.

In this paper, we obtain constraints on the coupling constants $g_{ap,p}$ and $g_{an,p}$ from measurements of the thermal Casimir-Polder force performed in Ref. [33]. Experiments on measuring the Casimir and Casimir-Polder forces have long been used for constraining the Yukawa-type corrections to Newtonian gravity mediated by light scalars or originating from extra-dimensional physics (see Ref. [34] for a review, and more recent results in Refs. [35–39]). These experiments, however, deal with the unpolarized test bodies. As to the potential arising between two fermions belonging to different test bodies from the exchange of a single axion with a pseudoscalar coupling, it is spin-dependent [29]. Thus, there is no net force in Casimir experiments due to a single axion exchange. It is not surprising, then, that

these experiments have not been used in the past to obtain constraints on the axion-like pseudoscalar particles. Nevertheless, a simultaneous exchange of two massless [40] or two massive [29] pseudoscalar particles between two fermions leads to a spin-independent interaction potential (this was used in Ref. [29] for constraining the parameters of an axion from the gravitational experiments of Eötvos- and Cavendish-type dealing with unpolarized test bodies). Here we use the same approach in application to the experiment on measuring the thermal Casimir-Polder force. The advantage of this experiment is that it was performed at comparatively large separation distances. We calculate the additional attractive force due to the exchange of two axions between fermions belonging to two test bodies in the experimental configuration. Then, from the fact that no extra force was observed in addition to the Casimir-Polder force in the limits of experimental errors, we arrive to novel stronger constraints on the coupling constants $g_{ap,p}$ and $g_{an,p}$. Our constraints are obtained in the region of axion masses from $100\,\mu$eV to $0.3\,$eV. Thus, these constraints extend those of Ref. [29] to a region important for astrophysics and cosmology.

The paper is organized as follows. In Sec. II, we calculate the attractive force which arises due to two-axion exchange in the experimental configuration of Ref. [33]. In Sec. III, we derive the constraints on the coupling constants $g_{ap,p}$ and $g_{an,p}$, which follow from the measure of agreement between the measurement data and theory. Section IV contains our conclusions and discussion. Below, we use the system of units with $\hbar = c = 1$.

II. ADDITIONAL FORCE ARISING FROM THE EXCHANGE OF TWO AXIONS IN EXPERIMENT ON MEASURING THERMAL CASIMIR-POLDER FORCE

A dynamic experiment demonstrating the thermal Casimir-Polder force acting between a cloud of approximately 2.5×10^5 ^{87}Rb atoms belonging to a Bose-Einstein condensate and a SiO_2 plate is described in Ref. [33]. A Bose-Einstein condensate was produced in a magnetic trap with frequencies $\omega_{0z} = 1438.85\,$rad/s and $\omega_{0t} = 40.21\,$rad/s in the perpendicular and lateral directions to the plate, respectively. The respective Thomas-Fermi radii of the condensate cloud were $R_z = 2.69\,\mu$m and $R_l = 97.1\,\mu$m. The back face of the SiO_2 plate was painted with $100\,\mu$m thick opaque layer of graphite and treated in a high temperature oven. By illuminating the graphite layer with laser light from an $860\,$nm laser, it was possible to

vary the temperature of the plate. The dipole oscillations of the condensate were excited with a constant amplitude $A_z = 2.5\,\mu$m in the z-direction (i.e., perpendicular to the plate). The temperature of the plate was either $T = 310\,$K (the same as the environment at the laboratory) or was increased to 479 K or 605 K. The separation between the plate and the cloud of ^{87}Rb atoms situated below it was varied from 6.88 to 11 μm. The influence of the Casimir-Polder force (or any additional force, i.e., due to the two-axion exchange) shifts the oscillation frequency in the z-direction from ω_{0z} to ω_z, and the relative frequency shift is given by

$$\gamma_z = \frac{|\omega_{0z} - \omega_z|}{\omega_{0z}} \approx \frac{|\omega_{0z}^2 - \omega_z^2|}{2\omega_{0z}^2}. \tag{1}$$

In Ref. [33], the frequency shift γ_z caused by the Casimir-Polder force was measured as a function of the separation a between the plate and the center of mass of the condensate. The absolute errors, $\Delta_i\gamma_z$, in the measurement of γ_z at different separations a_i have been found at a 67% confidence level [33].

It is possible to calculate the frequency shift in Eq. (1) under the influence of any force F acting between each atom of a condensate cloud and a plate (e.g., the Casimir-Polder force or the additional force due to two-axion exchange) averaged over the cloud. For this purpose, one can use the description of a dilute gas trapped by means of a harmonic potential and solve the mechanical problem with the result [33]

$$|\omega_{0z}^2 - \omega_z^2| = \frac{\omega_{0z}}{\pi A_z m_{\rm Rb}} \int_0^{2\pi/\omega_{0z}} d\tau \cos(\omega_{0z}\tau) \tag{2}$$
$$\times \int_{-R_z}^{R_z} dz n_z(z) F[a + z + A_z \cos(\omega_{0z}\tau)],$$

where $m_{\rm Rb}$ is the mass of ^{87}Rb atom and $n_z(z)$ is the distribution function of the atomic density in the z-direction [33]

$$n_z(z) = \frac{15}{16 R_z} \left(1 - \frac{z^2}{R_z^2}\right)^2. \tag{3}$$

To find the force F, acting between a ^{87}Rb atom and a SiO_2 plate due to two-axion exchange with a pseudoscalar coupling, we start with the respective interaction potential between two fermions k and l of spin 1/2 with masses m_k and m_l [29, 41, 42]

$$V(r) = -\frac{g_{ak,p}^2 g_{al,p}^2}{32\pi^3 m_k m_l} \frac{m_a}{r^2} K_1(2m_a r). \tag{4}$$

Here $g_{ak,p}$ and $g_{al,p}$ are the constants of a pseudoscalar axion-fermion interaction, $K_n(z)$ is the modified Bessel function of the second kind and it is assumed that $r \gg 1/m_{k(l)}$.

In the following, we disregard the interaction of axions with electrons [29]. The point is that in some axion models the axion-electron interaction does not exist at tree level and is only due to radiative corrections (in some other models there is the axion-electron coupling at tree level). In any case, the account of axion-electron interaction, or any interaction due to a scalar coupling of axion with fermions, could lead only to a minor increase of the magnitude of the additional force and, thus, only slightly strengthen the constraints obtained. Below, we consider the interaction of an atom with a plate situated above it due to two-axion exchange between protons and neutrons and put neutron and proton masses equal to $m = (m_n + m_p)/2$.

Using Eq. (4), the interaction potential of a ^{87}Rb atom with a SiO_2 plate can be obtained by the integration over the plate volume $V_{\rm pl}$

$$U = -\frac{\rho_{\rm SiO_2} m_a}{32\pi^3 m^2 m_{\rm H}}(37 g_{ap,p}^2 + 50 g_{an,p}^2) \times \left(\frac{Z_{\rm SiO_2}}{\mu_{\rm SiO_2}} g_{ap,p}^2 + \frac{N_{\rm SiO_2}}{\mu_{\rm SiO_2}} g_{an,p}^2\right) \int_{V_{\rm pl}} d^3 r \frac{1}{r^2} K_1(2m_a r). \tag{5}$$

Here, $\rho_{\rm SiO_2}$, $Z_{\rm SiO_2}$ and $N_{\rm SiO_2}$ are the density, the number of protons and the mean number of neutrons in a SiO_2 molecule, respectively. The quantity $\mu_{\rm SiO_2} = m_{\rm SiO_2}/m_{\rm H}$, where $m_{\rm SiO_2}$ and $m_{\rm H}$ are the mean mass of a SiO_2 molecule and the mass of an atomic hydrogen, respectively. It is also taken into account in Eq. (5) that ^{87}Rb atom contains 37 protons and 50 neutrons. The values of Z/μ and N/μ for the first 92 elements with account of their isotopic composition are given in Ref. [43]. For a SiO_2 molecule in accordance with Ref. [43] one finds

$$\frac{Z_{\rm SiO_2}}{\mu_{\rm SiO_2}} = \frac{Z_{\rm Si} + 2Z_{\rm O}}{\mu_{\rm Si} + 2\mu_{\rm O}} = 0.503205 \tag{6}$$

and

$$\frac{N_{\rm SiO_2}}{\mu_{\rm SiO_2}} = \frac{N_{\rm Si} + 2N_{\rm O}}{\mu_{\rm Si} + 2\mu_{\rm O}} = 0.505179. \tag{7}$$

In the experiment of Ref. [33] a SiO_2 plate of thickness $D = 7\,$mm and of large area $2 \times 10\,{\rm mm}^2$ has been used. Thus, all atoms of the condensate cloud can be approximately considered as situated below the plate center far away from its edges. Taking this into account, we can approximately replace the SiO_2 plate with a SiO_2 disc of $R = 1\,$mm radius and the same thickness D, as indicated above (below we estimate the role of the finiteness of the disc area and show that the plate can be replaced with a disc of infinitely large area at a very high accuracy). Now we introduce the cylindrical coordinates (ρ, φ, z), where the

z-axis begins at an atom located at a distance z below the plate and is directed to the plate. Then Eq. (5) takes the form

$$U = U(z) = -A(g_{ap,p}g_{an,p}) \int_z^{z+D} dz_1 \int_0^R \rho d\rho \times \frac{K_1(2m_a\sqrt{\rho^2+z_1^2})}{\rho^2+z_1^2}. \tag{8}$$

The factor A here is defined as

$$A(g_{ap,p}g_{an,p}) = \frac{\rho_{\rm SiO_2} m_a}{16\pi^2 m^2 m_{\rm H}}(37g_{ap,p}^2 + 50g_{an,p}^2) \times \left(\frac{Z_{\rm SiO_2}}{\mu_{\rm SiO_2}} g_{ap,p}^2 + \frac{N_{\rm SiO_2}}{\mu_{\rm SiO_2}} g_{an,p}^2\right). \tag{9}$$

From Eq. (8) we find the additional force acting on a ^{87}Rb atom due to the two-axion exchange

$$F_{\rm add}(z) = -\frac{\partial U(z)}{\partial z} = -A(g_{ap,p}g_{an,p}) \int_0^R \rho d\rho \times \left[\frac{K_1(2m_a\sqrt{\rho^2+z^2})}{\rho^2+z^2} - \frac{K_1(2m_a\sqrt{\rho^2+(z+D)^2})}{\rho^2+(z+D)^2}\right]. \tag{10}$$

It is convenient to use in Eq. (10) the following integral representation for the modified Bessel function [44]

$$K_1(t) = t\int_1^\infty e^{-tu}\sqrt{u^2-1}du. \tag{11}$$

By introducing the new variables $t = 2m_a\sqrt{\rho^2+z^2}$ and $t = 2m_a\sqrt{\rho^2+(z+D)^2}$ in the first and second terms on the right-hand side of Eq. (10), respectively, one obtains

$$\begin{aligned} F_{\rm add}(z) &= -A(g_{ap,p}, g_{an,p}) \int_1^\infty du\sqrt{u^2-1} \\ &\times \left[\int_{t_0^{(1)}}^{t_R^{(1)}} dte^{-tu} - \int_{t_0^{(2)}}^{t_R^{(2)}} dte^{-tu}\right] \\ &= -A(g_{ap,p}, g_{an,p}) \int_1^\infty du \frac{\sqrt{u^2-1}}{u} \\ &\times \left[e^{-t_0^{(1)}u} - e^{-t_R^{(1)}u} - e^{-t_0^{(2)}u} + e^{-t_R^{(2)}u}\right], \end{aligned} \tag{12}$$

where the following notations are introduced:

$$\begin{aligned} t_0^{(1)} &= 2m_a z, \qquad t_R^{(1)} = 2m_a\sqrt{R^2+z^2}, \\ t_0^{(2)} &= 2m_a(z+D), \qquad t_R^{(2)} = 2m_a\sqrt{R^2+(z+D)^2}. \end{aligned} \tag{13}$$

Now we are in a position to calculate the additional frequency shift (1) originating from the two-axion exchange between atoms of the condensate cloud and the plate. For this purpose, we substitute $F_{\rm add}$ from Eq. (12) in place of F in Eq. (2). Let us first calculate the contribution $\gamma_{z,1}^{\rm add}$ into $\gamma_z^{\rm add}$ which originates from the first and third terms on the right-hand side of Eq. (12). For these terms, the integration with respect to τ in Eq. (2) (i.e., the averaging over the oscillator period) and with respect to z (i.e., the averaging over the condensate cloud) can be performed exactly in close analogy to Ref. [35], giving, as a result,

$$\gamma_{z,1}^{\rm add}(a)=\frac{15A(g_{ap,p},g_{an,p})}{2\pi A_z m_{\rm Rb}\omega_{0z}^2}\int_1^\infty du\frac{\sqrt{u^2-1}}{u}e^{-2m_a au} \times\left(1-e^{-2m_aDu}\right)I_1(2m_aA_zu)\Theta(2m_aR_zu). \tag{14}$$

Here, we have introduced the notation

$$\Theta(t)\equiv\frac{1}{t^3}(t^2\sinh t-3t\cosh t+3\sinh t). \tag{15}$$

We emphasize that the quantity in Eq. (14) coincides with the total relative frequency shift arising from the interaction of a condensate cloud with a disc of an infinitely large radius $R\to\infty$.

In order to perform the averaging over the oscillation period and over the condensate cloud of the second and fourth terms on the right-hand side of Eq. (12) (these terms describe the boundary effects due to finiteness of plate area), we take into account that, in our problem, $z\ll R$ (specifically, $z/R<10^{-2}$) and use the following expansions:

$$\begin{aligned}
t_R^{(1)}&\approx 2m_aR+m_a\frac{z^2}{R},\\
t_R^{(2)}&\approx 2m_a\sqrt{R^2+D^2}+\frac{2m_aD}{\sqrt{R^2+D^2}}z,\\
e^{-t_R^{(1)}u}&\approx e^{-2m_aRu}\left(1-m_a\frac{z^2}{R}u\right),\\
e^{-t_R^{(2)}u}&\approx e^{-2m_a\sqrt{R^2+D^2}u}\left(1-\frac{2m_aDz}{\sqrt{R^2+D^2}}u\right).
\end{aligned} \tag{16}$$

After calculations with acount of Eq. (16), the contribution of the second and fourth terms to the additional frequency shift takes the form

$$\gamma_{z,2}^{\rm add}(a)=-\frac{15A(g_{ap,p},g_{an,p})m_a}{8m_{\rm Rb}\omega_{0z}^2} \times\left[\frac{a}{R}\int_1^\infty du\sqrt{u^2-1}e^{-2m_aRu} +\frac{D}{\sqrt{R^2+D^2}}\int_1^\infty du\sqrt{u^2-1}e^{-2m_a\sqrt{R^2+D^2}u}\right]. \tag{17}$$

Calculating the integrals in Eq. (17) we arrive at

$$\gamma_{z,2}^{\rm add}(a)=-\frac{15A(g_{ap,p},g_{an,p})}{16m_{\rm Rb}\omega_{0z}^2} \times\left[\frac{a}{R^2}K_1(2m_aR)+\frac{D}{R^2+D^2}K_1(2m_a\sqrt{R^2+D^2})\right]. \tag{18}$$

Finally, by adding Eqs. (14) and (18), we obtain the total additional frequency shift due to the exchange of two axions with pseudoscalar couplings between protons and neutrons of a condensate and a plate:

$$\gamma_{z}^{\rm add}(a)=\frac{15A(g_{ap,p},g_{an,p})}{2\pi A_zm_{\rm Rb}\omega_{0z}^2}\Phi(a,m_a), \tag{19}$$

where

$$\Phi(a,m_a)=\int_1^\infty du\frac{\sqrt{u^2-1}}{u}e^{-2m_aau} \times\left(1-e^{-2m_aDu}\right)\,I_1(2m_aA_zu)\Theta(2m_aR_zu) -\frac{\pi A_za}{8R^2}K_1(2m_aR)-\frac{\pi A_zD}{8(R^2+D^2)}K_1(2m_a\sqrt{R^2+D^2}). \tag{20}$$

It is interesting to estimate the role of boundary effects due to a finiteness of the disc represented by the quantity $\gamma_{z,2}^{\rm add}(a)$ in Eq. (18). Computations show that over the entire measurement range $6.88\,\mu{\rm m}\leq a\leq 11\,\mu{\rm m}$ and for all axion masses m_a from $100\,\mu$eV to $0.3\,$eV considered below the following holds:

$$\left|\frac{\gamma_{z,2}^{\rm add}(a)}{\gamma_{z,1}^{\rm add}(a)}\right|<10^{-6}. \tag{21}$$

This demonstrates that the boundary effects are negligibly small and the additional frequency shift (19) due to the two-axion exchange can be calculated with sufficient precision by using the first term on the right-hand side of Eq. (20).

III. CONSTRAINTS ON THE PSEUDOSCALAR COUPLINGS BETWEEN AXION AND NUCLEONS

In the experiment of Ref. [33] the measured frequency shifts were found to be in agreement with the calculated frequency shifts caused by the Casimir-Polder force between ^{87}Rb atoms of a condensate cloud and a SiO_2 plate. The Casimir-Polder force was calculated [33] by using the standard Lifshitz theory [34, 45] in an equilibrium situation (when the temperatures of

a plate and of the environment were equal) and its generalization [46] for a nonequilibrium case (when the plate was hoter than the environment). In both cases, computations of the Casimir-Polder force were performed by omitting the conductivity of a SiO_2 plate at a constant current. The crucial role of this omission was underlined in Ref. [47] (see also review of subsequent discussions in Ref. [48]).

Agreement between the measured and calculated frequency shifts caused by the Casimir-Polder force was achieved in the limits of experimental errors $\Delta_i\gamma_z$. This means that any additional frequency shift is restricted by the inequality

$$\gamma_z^{\rm add}(a_i) \leq \Delta_i\gamma_z, \tag{22}$$

where a_i are the separation distances at which the measurements of Ref. [33] were performed. Now we substitute Eqs. (19) and (20) in Eq. (22) and obtain the respective constraints on the coupling constants $g_{ap,p}$, $g_{an,p}$ and the axion mass m_a. For this purpose, it is convenient to use Eqs. (6), (7), (9) and rewrite Eqs. (19) and (20) in the form

$$\gamma_z^{\rm add}(a) = \left(\frac{g_{an,p}^2}{4\pi}+\frac{0.503205}{0.505179}\,\frac{g_{ap,p}^2}{4\pi}\right) \times\left(\frac{g_{an,p}^2}{4\pi}+\frac{37}{50}\,\frac{g_{ap,p}^2}{4\pi}\right)\chi(a,m_a), \tag{23}$$

where

$$\chi(a,m_a)=\frac{189.442\rho_{\rm SiO_2}m_a}{\pi A_z m_{\rm Rb}m_{\rm H}m^2\omega_{0z}^2}\,\Phi(a,m_a). \tag{24}$$

Then Eq. (22) can be rewritten as

$$\frac{g_{an,p}^4}{16\pi^2}+1.73609\frac{g_{ap,p}^2g_{an,p}^2}{16\pi^2}+0.737108\frac{g_{ap,p}^4}{16\pi^2}-\frac{\Delta_i\gamma_z}{\chi(a_i,m_a)}\leq 0. \tag{25}$$

We have numerically analyzed Eq. (25) at different experimental points (i.e., for different values of a_i and $\Delta_i\gamma_z$) and within different ranges of the axion mass m_a. The strongest constraints on the quantities $g_{an,p}^2/4\pi$ and $g_{ap,p}^2/4\pi$ over the region of axion masses $m_a > 10\,{\rm meV}$ follow from the measurement set in thermal equilibrium at the separation distance $a_1=6.88\,\mu{\rm m}$, with an absolute error $\Delta_1\gamma_z=3.06\times10^{-5}$ determined at a 67% confidence level [33]. As an example, in Fig. 1 we plot the obtained constraints for $m_a=0.2\,{\rm eV}$ as an upper line in the plane $(g_{ap,p}^2/4\pi, g_{an,p}^2/4\pi)$, where the region of the plane above the line is excluded by the results of this experiment at the 67% confidence level and the region below the line is allowed. As can be seen in Fig. 1, the largest possible value of $g_{ap,p}^2/4\pi=2.23\times10^{-2}$

is much larger than the respective $g^2_{an,p}/4\pi$. In a similar way, the largest possible value of $g^2_{an,p}/4\pi$ for the axion with $m_a = 0.2\,\mathrm{eV}$ is equal to 1.91×10^{-2} and it is much larger than the respective $g^2_{ap,p}/4\pi$.

For small axion masses $m_a \leq 0.01\,\mathrm{eV}$ the strongest constraints follow from the out of thermal equilibrium measurements of Ref. [33], where the plate temperature $T = 479\,\mathrm{K}$ was higher than the temperature of an environment ($T = 310\,\mathrm{K}$). The strongest constraints here are obtained at $a_2 = 7.44\,\mu\mathrm{m}$, where the experimental error determined at a 67% confidence level is equal to $\Delta_2\gamma_z = 2.35 \times 10^{-5}$ [33]. In Fig. 1, we show the obtained constraints for $m_a = 0.01\,\mathrm{eV}$ and for $m_a \leq 1\,\mathrm{meV}$ by the intermediate and lower lines, respectively. Note that further decrease of m_a does not lead to further strengthening of the constraints obtained from this experiment. For the intermediate line ($m_a = 0.01\,\mathrm{eV}$) the largest possible values of the coupling constants are $g^2_{ap,p}/4\pi = 5.76 \times 10^{-4} \gg g^2_{an,p}/4\pi$ and $g^2_{an,p}/4\pi = 4.86 \times 10^{-4} \gg g^2_{ap,p}/4\pi$. For axions of lower mass ($m_a \leq 1\,\mathrm{meV}$), the largest possible values of the coupling constants with hadrons are $g^2_{ap,p}/4\pi = 4.97 \times 10^{-4} \gg g^2_{an,p}/4\pi$ and $g^2_{an,p}/4\pi = 4.20 \times 10^{-4} \gg g^2_{ap,p}/4\pi$, respectively.

It is of interest also to find the constraints on the coupling constants of an axion to a proton and to a neutron as functions of the axion mass m_a. This can be also done by using Eq. (25) under different assumptions about the relationship between $g_{ap,p}$ and $g_{an,p}$. In Fig. 2, the lower line shows the constraints on $g_{ap,p} = g_{an,p}$ over a wide region of axion masses from 0.1 meV to 0.3 eV. The intermediate and upper lines show the constraints on $g_{ap,p}$ under the condition $g_{ap,p} \gg g_{an,p}$ and on $g_{an,p}$ under the condition $g_{an,p} \gg g_{ap,p}$, respectively. As can be seen in Fig. 2, the obtained constraints become stronger when the axion mass decreases from $m_a = 0.3\,\mathrm{eV}$ to $m_a = 1\,\mathrm{meV}$. With further decrease of an axion mass, the strength of constraints remains almost constant (similar to Fig. 1, the region of the plane above each line is excluded at a 67% confidence level by measurements of the thermal Casimir force and the region below each line is allowed).

We now compare the constraints of Figs. 1 and 2 with previous constraints on the parameters of the axion-like particles obtained from laboratory experiments. The constraints of Ref. [29] on the coupling constant $g^2_{an,p}/4\pi$ are obtained from the Cavendish-type experiment [28] under an assumption $g^2_{ap,p} = 0$ for axion masses $m_a \leq 2 \times 10^{-5}\,\mathrm{eV}$. Thus, it is not possible to perform direct comparison with our constraints obtained for $m_a \geq 10^{-4}\,\mathrm{eV}$. If, however, one extrapolates the constraints of Ref. [29] to larger m_a, our constraints shown by

the upper line in Fig. 2 become stronger for axion masses $m_a > 0.4\,\mathrm{meV}$ (this corresponds to the Compton wavelength of an axion $\lambda_a < 0.5\,\mathrm{mm}$). The other laboratory constraints are obtained [29, 49] from the Eötvos-type experiment [26] combined with the study of laser beam propagation through a transverse magnetic field [50] for axion masses $m_a \leq 1\times 10^{-5}\,\mathrm{eV}$. They also cannot be directly compared with our constraints. The extrapolation of the constraints of Refs. [29, 49] to larger m_a becomes weaker than our constraints shown by the upper line in Fig. 2 for axion masses $m_a > 0.04\,\mathrm{meV}$ (i.e., $\lambda_a < 5\,\mathrm{mm}$). Thus, our results present the model-independent laboratory limits on the nucleon coupling constants of axions which are most strong in the region from $m_a = 10^{-4}\,\mathrm{eV}$ to $m_a = 10\,\mathrm{meV}$.

IV. CONCLUSIONS AND DISCUSSION

In the foregoing we have considered the parameters of the axion-like particles and constrained the pseudoscalar coupling constants of such particles with proton and neutron from the measurement data of a recent experiment [33] on measuring the thermal Casimir-Polder force between a condensate cloud of ^{87}Rb atoms and a SiO_2 plate. It was stressed that the axion provides the most natural way for the resolution of two fundamental problems of modern physics. One of them is the problem of *CP* violation in quantum chromodynamics and another one is the problem of dark matter in astrophysics and cosmology. Because of this, any additional information about the coupling constants and the mass of the axion is of much value for further experimental search for this particle.

We have underlined that laboratory experiments for searching the axion and other axion-like particles are more model-independent than the numerous results found from different cosmological scenaria, astrophysics and astronomical observations. Unfortunately, the already performed gravitational and optical laboratory experiments are only sensitive to axions of very small masses less or of order of $10\,\mu\mathrm{eV} = 10^{-2}\mathrm{meV}$. However, all kinds of experiments and observations combined together indicate that the upper limit for the axion mass may be of about $m_a \approx 10\,\mathrm{meV}$ [1]. In this paper we have shown that measurements of the thermal Casimir-Polder force place strong constraints on the pseudoscalar coupling constants of an axion with a proton and a neutron in the wide region of axion masses from 0.1 meV to 0.3 eV. This region overlaps significantly with the so-called *axion window* which extends from $10^{-2}\,\mathrm{meV}$ to $10\,\mathrm{meV}$.

The results obtained demonstrate that laboratory experiments on measuring the Casimir force can be used not only for constraining the Yukawa-type hypothetical interactions caused by the exchange of scalar particles or inspired by extra dimensions, but for placing limits on the parameters of the axion-like particles as well. For this reason in the future it is pertinent to analyze all already performed experiments on measuring the Casimir force [48] and to elaborate some optimum configuration for the measurement of the Casimir force best suited for obtaining the strongest constraints on the parameters of the axion.

Acknowledgments

This work was partially supported by CNPq (Brazil). G.L.K. and V.M.M. are grateful to M. I. Eides for helpful discussions. They also acknowledge the Department of Physics of the Federal University of Paraíba (João Pessoa, Brazil) for hospitality.

---

[1] J. Beringer *et al.* (Particle Data Group), Phys. Rev. D **86**, 010001 (2012).

[2] R. D. Peccei and H. R. Quinn, Phys. Rev. Lett. **38**, 1440 (1977).

[3] S. Weinberg, Phys. Rev. Lett. **40**, 223 (1978).

[4] F. Wilczek, Phys. Rev. Lett. **40**, 279 (1978).

[5] J. Preskill, M. B. Wise, and F. Wilczek, Phys. Lett. B **120**, 127 (1983).

[6] L. F. Abbott and P. Sikivie, Phys. Lett. B **120**, 133 (1983).

[7] P. Sikivie, Phys. Rev. Lett. **51**, 1415 (1983).

[8] M. Dine and W. Fischler, Phys. Lett. B **120**, 137 (1983).

[9] R. L. Davis, Phys. Lett. B **180**, 225 (1986).

[10] J. E. Kim, Phys. Rep. **150**, 1 (1987).

[11] J. E. Moody and F. Wilczek, Phys. Rev. D **30**, 130 (1984).

[12] L. J. Rosenberg and K. A. van Bibber, Phys. Rep. **325**, 1 (2000).

[13] G. G. Raffelt, J. Phys. A: Math. Theor. **40**, 6607 (2007).

[14] J. E. Kim and G. Carosi, Rev. Mod. Phys. **82**, 557 (2010).

[15] G. Raffelt, Phys. Rev. D **86**, 015001 (2012).

[16] M. Arik *et al.*, Phys. Rev. Lett. **107**, 261302 (2011).

[17] G. G. Raffelt, *Stars as Laboratories for Fundamental Physics* (University of Chicago Press, Chicago, 1996).

[18] G. G. Raffelt, Phys. Rev. D **33**, 897 (1986).

[19] H. Schlattl, A. Weiss, and G. Raffelt, Astropart. Phys. **10**, 353 (1999).

[20] M. Kawasaki and K. Nakayama, Annu. Rev. Nucl. Part. Sci. **63**, 69 (2013).

[21] D. Cadamuro, S. Hannestad, G. Raffelt, and J. Redondo, J. Cosmol. Astropart. Phys. **02**, 003 (2011).

[22] J. Jaeckel, E. Massó, J. Redondo, A. Ringwald, and F. Takahashi, Phys. Rev. D **75**, 013004 (2007).

[23] P. Brax, C. van de Bruck, and A.-C. Davis, Phys. Rev. Lett. **99**, 121103 (2007).

[24] E. Fischbach and D. E. Krause, Phys. Rev. Lett. **82**, 4753 (1999).

[25] E. Fischbach and D. E. Krause, Phys. Rev. Lett. **83**, 3593 (1999).

[26] G. L. Smith, C. D. Hoyle, J. H. Gundlach, E. G. Adelberger, B. R. Heckel, and H. E. Swanson, Phys. Rev. D **61**, 022001 (1999).

[27] J. H. Gundlach, G. L. Smith, E. G. Adelberger, B. R. Heckel, and H. E. Swanson, Phys. Rev. Lett. **78**, 2523 (1997).

[28] R. Spero, J. K. Hoskins, R. Newman, J. Pellam, and J. Schultz, Phys. Rev. Lett. **44**, 1645 (1980).

[29] E. G. Adelberger, E. Fischbach, D. E. Krause, and R. D. Newman, Phys. Rev. D **68**, 062002 (2003).

[30] B. R. Heckel, C. E. Cramer, T. S. Cook, E. G. Adelberger, S. Schlamminger, and U. Schmidt, Phys. Rev. Lett. **97**, 021603 (2006).

[31] S. A. Hoedl, F. Fleischer, E. G. Adelberger, and B. R. Heckel, Phys. Rev. Lett. **106**, 041801 (2011).

[32] S. A. Hoedl, E. G. Adelberger, and B. R. Heckel, Physics Procedia **17**, 96 (2011).

[33] J. M. Obrecht, R. J. Wild, M. Antezza, L. P. Pitaevskii, S. Stringari, and E. A. Cornell, Phys. Rev. Lett. **98**, 063201 (2007).

[34] M. Bordag, G. L. Klimchitskaya, U. Mohideen, and V. M. Mostepanenko, *Advances in the Casimir Effect* (Oxford University Press, Oxford, 2009).

[35] V. B. Bezerra, G. L. Klimchitskaya, V. M. Mostepanenko, and C. Romero, Phys. Rev. D **81**, 055003 (2010).

[36] V. B. Bezerra, G. L. Klimchitskaya, V. M. Mostepanenko, and C. Romero, Phys. Rev. D **83**, 075004 (2011).

[37] G. L. Klimchitskaya, U. Mohideen, and V. M. Mostepanenko, Phys. Rev. D **86**, 065025 (2012).

[38] V. M. Mostepanenko, V. B. Bezerra, G. L. Klimchitskaya, and C. Romero, Int. J. Mod. Phys. A **27**, 1260015 (2012).

[39] G. L. Klimchitskaya, U. Mohideen, and V. M. Mostepanenko, Phys. Rev. D **87**, 125031 (2013).

[40] V. M. Mostepanenko and I. Yu. Sokolov, Sov. J. Nucl. Phys. **46**, 685 (1987).

[41] S. D. Drell and K. Huang, Phys. Rev. **91**, 1527 (1953).

[42] F. Ferrer and M. Nowakowski, Phys. Rev. D **59**, 075009 (1999).

[43] E. Fischbach and C. L. Talmadge, *The Search for Non-Newtonian Gravity* (Springer, New York, 1999).

[44] I. S. Gradshtein and I. M. Ryzhik, *Table of Integrals, Series and Products* (Academic Press, New York, 1980).

[45] E. M. Lifshitz and L. P. Pitaevskii, *Statistical Physics*, Part II (Pergamon, Oxford, 1980).

[46] M. Antezza, L. P. Pitaevskii, and S. Stringari, Phys. Rev. A **70**, 053619 (2004).

[47] G. L. Klimchitskaya and V. M. Mostepanenko, J. Phys. A: Math. Theor. **41**, 312002 (2008).

[48] G. L. Klimchitskaya, U. Mohideen, and V. M. Mostepanenko, Rev. Mod. Phys. **81**, 1827 (2009).

[49] E. Massó, Phys. Rev. D **61**, 011701(R) (1999).

[50] R. Cameron, G. Cantatore, A. C. Melissinos, G. Ruoso, Y. Semertzidis, H. J. Halama, D. M. Lazarus, and A. G. Prodell, Phys. Rev. D **47**, 3707 (1993).

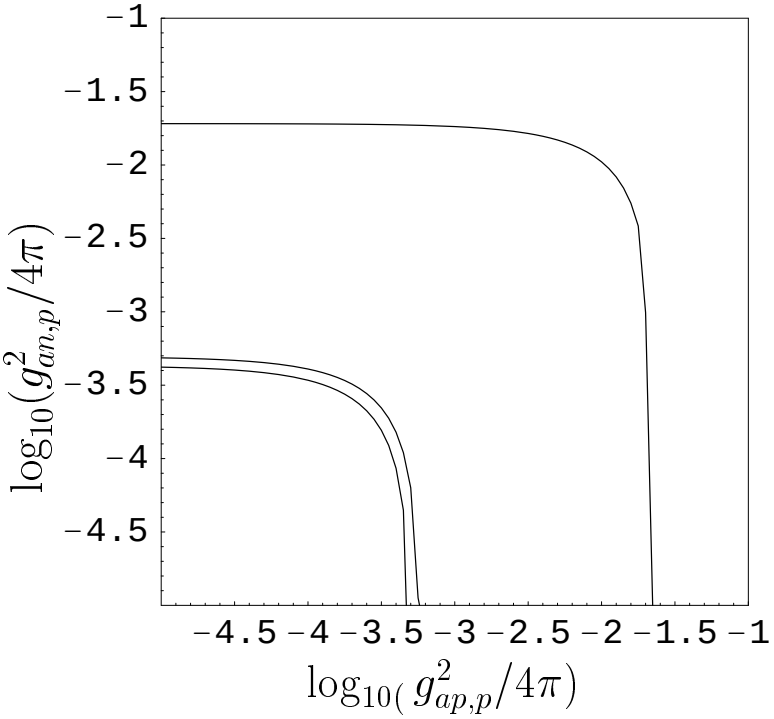

FIG. 1: Constraints on the pseudoscalar coupling constants of an axion with a proton and a neutron following from measurements of the thermal Casimir-Polder force are shown as the upper, intermediate and lower lines for the axion masses $m_a = 0.2\,\text{eV}$, $0.01\,\text{eV}$ and $\leq 1\,\text{meV}$, respectively (see text for further discussion). The regions of the plane above each line are prohibited and below each line are allowed.

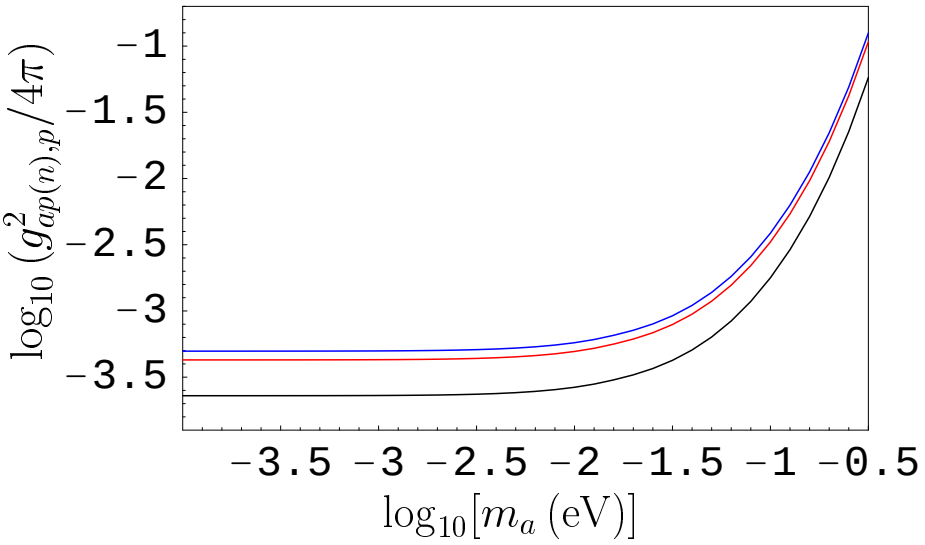

FIG. 2: (Color online) Constraints on the pseudoscalar coupling constants of an axion with a proton or a neutron following from measurements of the thermal Casimir-Polder force are shown as functions of the axion mass. The lower, intermediate and upper lines correspond to the conditions $g_{ap,p} = g_{an,p}$, $g_{ap,p} \gg g_{an,p}$, and $g_{an,p} \gg g_{ap,p}$, respectively. The regions of the plane above each line are prohibited and below each line are allowed.